ON THE BOUNDARY VALUE KIRSCH'S PROBLEM

D. Rezini * **A. Khaldi** **Y. Rahmani**

Université des Sciences et de la Technologie Mohamed Boudiaf
Oran, Algérie

ABSTRACT

Analytical closed-form solution to the stress distribution associated with a hole in finite plates subjected to tension has not been obtained yet. Wherefore, a method developed in this paper is based on a Beltrami-Michell methodology analyzing the Kirsch's problem under finite dimensions conditions of both plane stress and plane strain. This aimed ability is achieved by combining the Beltrami-Michell plane equations, isochromatic information on the boundaries only; and the finite difference method into an effectual hybrid method for analyzing rectangular plates of finite width with circular holes. Furthermore, the Beltrami-Michell methodology suggested may be applied on other plate and cut-out forms.

Keywords: Kirsch's problem, Dirichlet, Photoelasticity, Hybrid method.

1. INTRODUCTION

Analytical and experimental analysis showed that near openings in a loaded flat member a peak stress occurs, which reaches much larger magnitudes than does the average stress over the section. Therefore, a stress field disturbance occurs round about. First of all, Kirsch [1] published a pioneering work on the stress state of a uniaxially tensioned elastic plane which is weakened by a circular hole. Acknowledged as *Kirsch's problem*, this work was the beginning of a new direction in the plane theory of elasticity. His ideas were further developed by the Russian mathematician Kolosov [2] who initiated the stress concentration study around arbitrary shaped holes and size in elastic medium, which is subjected to diverse loading conditions. Hereafter, Inglis [3] accomplished the work of Kolosov and has obtained an analytical solution associated with an elliptical hole. Finally, two further important problems are treated, which are fundamental ideas of fracture mechanics. Earlier on, Howland [4] analyzed the stresses in the neighbourhood of a circular hole, and he suggested a formulation for calculation of the stress concentration factors of an isotropic strip with circular holes. Over the years different techniques have been developed for the study of such weakened plates. Thereafter, the stress distribution was studied around both circular (Durelli *et al.* [5]) and elliptical discontinuity (Durelli *et al.* [6]) using, among others, photoelasticity. Additionally, much experimental work related to this topic has contributed to validate the analytical solutions [7]. Most recently, for other shapes of holes Kawadkar [8], for example, proposes an evaluation of stress concentration in plate with cut-out and its experimental verification. Furthermore, a study on the effect of stress concentration on cut-out orientation of plates with various cut-outs and bluntness was conducted by Mohan [9]. Numerous of papers can by cited concerning solutions for stress concentration around holes [10,11]. Studies of elastic stress in infinite plate weakened by a single circular hole have been published by Singh [12], in comparison with those weakened by multiple circular holes [13]. Furthermore, finite element analyses are performed to investigate elastic stresses around holes in plate subjected to uniform tensile loading, as published by Shastry *et al.* [14]. Semi-analytical and experimental work also exists for finite width plates [15], and for finite thickness plates. Indeed, on the basis of the plane strain theory, Kotousov [16] presented analytical solutions for a wide range of thickness to radius ratios around typical stress concentrators in an isotropic plate with arbitrary thickness. However, Yang *et al.* [17] showed that the location of stress raiser occurs on the middle surface only in thin plates and it moves away from the mid plane of plate by increasing the plate thickness. To abbreviate this bibliographical review, an exhaustive review on stress analysis of an infinite plate with cut-outs is edited by Dharmin *et al.* [18], where contributions of work from several researchers have been recapitulated. Besides, an extensive collection of stress concentration factors, in table-forms ready for use, is provided in textbooks, as compiled by Pilkey [19].

There are various theories and techniques commonly used for this purpose, some of which have been listed above. Some problems have been solved using series method [20], as introduced early by Love [21]. Abdou and Monaquel have used an integral method to determine the stress components of stretched infinite plate with a curvilinear hole [22]. Various numerical pro-

* Corresponding author (redjellou@yahoo.fr)

DOI : 10.1017/jmech.2015.93
Copyright © 2015 The Society of Theoretical and Applied Mechanics, R.O.C.
https://doi.org/10.1017/jmech.2015.93 Published online by Cambridge University Press

cedures (Finite and Boundary Element Methods) have been developed to get solutions to elasticity problems of complex geometry. The most important method used in several papers is based on the complex variables theory introduced previously by Kolosov followed by other authors such as Churchill [23] and England [24]. Several authors have formulated perturbed two-dimensional problem in terms of Savin's complex variable method [25] or, as a hybrid version, Muskhelishvili's complex variable method [26] and the finite element method.

The main concern of this paper is to separate, in several components, the perturbed stress field due to the peak stress. Unfortunately, the occurred stress concentrations on the edges cannot be determined, since they are designed as boundary values of the problem that is owing to the boundary value problem conceptual formulation. It must be emphasized that the above literature review does not suggest any work that has been done to investigate the perturbed stress field in its boundary value problem version. To our knowledge, no work has not been obtained yet to examine weakened finite width domain, as a stress boundary value problem. Therefore, the designed methodology should be an efficient alternative procedure for plane stress analysis, because based on the Beltrami-Michell stress formulation. In addition, the methodology shall be capable of mapping two-dimensional stress tensor components within plates of finite-width weakened by holes more efficiently (Ref. to [18]), with results that are sufficiently accurate for engineering design purposes.

The suggested Beltrami-Michell methodology is organized as follows. The source functions of the Beltrami-Michell equations from Poisson-Type can take second order partial derivatives either homogeneous or mixed of the stress sum function. The first stress tensor invariant as harmonic function, satisfying Laplace equation can be determined throughout the planar domain from known surface stress sum [27]. Thus, the first Dirichlet problem must be solved at first. Chained up, the second operation of the problem is to build second order derivatives of the stress sum function, which express each source functions of the Beltrami-Michell compatibility equations. The third operation therefore is to solve the Beltrami-Michell Boundary Value Problem (BM-BVP) [28]. So, the second Dirichlet problem, in terms of stress tensor components, could be solved at last. In both cases, the required Dirichlet data may be determined by means of any method that permits to measure surface stresses; among others photoelasticity is the most designated [29,30]. This aimed ability is achieved by combining isochromatic information on the boundaries solely, the B-M BVP and the Finite Difference Method (FDM), into an effectual hybrid method for stress analysis [31]. In order to show the versatility of the proposed method, the first application on the Kirsch problem enables the comparison of the present results with analytical ones. The second application concerns a photoelastic finite plate that allows the comparison with the experimental ones; and to show furthermore the superiority of the suggested method.

2. BELTRAMI-MICHELL BOUNDARY VALUE STRESS PROBLEM

This section reviews and illustrates the compatibility requirement of the in plane elasticity theory. It is worth noting that the field equations for plane stress are almost identical to those for plane strain, except for the term involving Poisson's ratio in the constitutive law. However, the equations of equilibrium, which are the same for plane stress and plane strain, are given by:

$$\begin{aligned} \frac{\partial \sigma_{xx}}{\partial x}+\frac{\partial \sigma_{xy}}{\partial y}+X=0 \\ \frac{\partial \sigma_{yy}}{\partial y}+\frac{\partial \sigma_{xy}}{\partial x}+Y=0 \end{aligned} \tag{1}$$

where, X and Y are body forces. In the field, the equilibrium equations are functionally indeterminate because three unknown stresses are expressed in terms of two Eq. (1). The requirement of compatible strains in the plane may form the third equation used for the determination of all the stress components. Indeed, there are three strain equations for the determination of two unknown displacement functions in the plane. Accordingly, the following is also to be noted, with the assumption that the in-plane displacement components are single-valued and have continuous derivatives up to and including the third order. Hence the given components of strain must likewise be single-valued and have continuous derivatives of the second order; this condition will be assumed to be satisfied. Consequently, the three strains, ε_{xx}, ε_{yy} and γ_{xy}, which are of interest in the plane stress and plane strain problems, are not independent. The following equation expresses this fact:

$$\frac{\partial^2 \varepsilon_{yy}}{\partial x^2}+\frac{\partial^2 \varepsilon_{xx}}{\partial y^2}=\frac{\partial^2 \gamma_{xy}}{\partial x \partial y} \tag{2}$$

Equation (2) is the condition of compatibility and must be satisfied in order to ensure the integrability of the strains to obtain single valued displacements. The compatibility equation puts a condition on the stresses since the strains calculated from them must satisfy (1). Expressing the strains in terms of the stresses by means of Hooke's law for plane stress,

$$\varepsilon ij=-\frac{\nu}{E}\sigma kk\delta ij+\frac{1+\nu}{E}\sigma ij \tag{3}$$

substituting in Eq. (2) and eliminating the shear stress, σ_{xy}, by means of the equilibrium Eq. (1), the standard form of the Beltrami-Michell compatibility equation (B-MCE) may be obtained:

$$\Delta I_\sigma(x, y)=\Delta(\sigma_{xx}+\sigma_{yy})=0 \tag{4}$$

where the trace of the plane stress tensor $I_\sigma(x, y)$ is used, and the Laplace operator is symbolized by Δ. It must emphasized, however, that if there is no volume force, then the B-MCE (4) has the same form for both plane states. This postulate may be easily verified by taking

https://doi.org/10.1017/jmech.2015.93 Published online by Cambridge University Press

into account plane strain assumptions (*i.e.* $\varepsilon_{zz} = 0$; $\sigma_{zz} = \nu(\sigma_{xx} + \sigma_{yy} + E_{e0})$), where e_0 is the constant axial strain which is independent of stress. In this case a normal stress σ_{zz} exists in addition to the other three components. Therefore, the stress invariant for plane strain conditions, $I_\sigma(x, y) = (1 + \nu)(\sigma_{xx} + \sigma_{yy}) + E_{e0}$, to which the contribution of Laplacian will lead to the B-MCE shown in (4) above. It is worth noting that the resulting equation is valid for both plane stress and plane strain, since material constants have disappeared, and there is thus no need to use the formal equivalence between plane stress and plane strain.

The two equilibrium Eq. (1) and the *material constant free* B-MCE (4), for plane stress or plane strain, are sufficient to determine the stresses when the boundary conditions are specified. Moreover, the solution of an elasticity plane problem may be reduced to the search of the solution of its boundary value problem. Whereby, we shall consider only those solutions in which the stress tensor components are continuous and single-valued throughout the region, Ω, together with their first and second partial derivatives with respect to x and y.

Remark: There are several stress separation methods available for two dimensional problems, and which are used with some reservation. Hence, the challenge is still ahead in the development of techniques with better performances. Customarily, the sum of the stresses, $(\sigma_{xx} + \sigma_{yy})$, field solution of the Dirichlet's problem (4) is used for the stress-separation, involving one of both equilibrium equations in an integration procedure, provided that the shear stress, σ_{xy}, is known on the path. For a full-field stresses separation, this procedure will be repeated, line-by-line, until the three different stress maps are generated. Other methods reach such a stresses separation using simultaneous both normal stress difference, $(\sigma_{xx} - \sigma_{yy})$, and the normal stress sum solution, (4), assuming also that the shear stress is eventually available in the field. It is to emphasize that both methods need for this purpose photoelastic information in the field; a huge and tedious task at last. It would be still more preferable to determine each components of the stress tensor separated, without use of information within the field. However, an still more efficient alternative will be developed in this paper.

The highlighted aim of this study is to try to transform Eq. (4) in such a way that the stress separation occurs, arising from the determination of each individual stress component in the field.

We shall use for the convenience purpose the Airy stress function, ϕ, which has been used also by Kirsch [1] to find the solution to his problem (see section 4). It will be shown, that this leads straight to the proper B-MCE governing the plan version. While the Eq. (1) represent a necessary and sufficient condition for the existence of a Airy stress function $\phi(x, y)$, consequently, the three components of the symmetrical stress tensor may be expressed through this single Airy function, such that:

$$\sigma(\phi) = \begin{pmatrix} \dfrac{\partial^2 \phi}{\partial y^2} & -\dfrac{\partial^2 \phi}{\partial x \partial y} \\ sym. & \dfrac{\partial^2 \phi}{\partial x^2} \end{pmatrix} \tag{5}$$

In addition, the first invariant or trace of the stress tensor

$$I_\sigma(x, y) = \sigma_{xx} + \sigma_{yy} = \Delta\phi \tag{6}$$

has all the properties of a harmonic function what satisfies the Laplace equation. By taking the Laplacian, Δ, of both sides of the Eq. (6), we get both a Laplace and a bi-Laplace equation:

$$\Delta I_\sigma(x, y) = \Delta\Delta\phi = 0 \tag{7}$$

These equations express both the B-MCE and the bi-harmonic compatibility equation in terms of the stress function for the two dimensional case of course. The requirement that the elastic domain, Ω being simply-connected, is needed to ensure that $\phi(x, y)$ is single-valued. Multiply connected domains also have a single valued, ϕ, provided that the integrals of the equilibrium equations (force and torque) vanish separately on each internal boundary of cut-outs (refer to [26]). Thus, this theorem states that the stresses in a doubly connected plate (*of Kirsch*), induced by specified tractions, do not depend on the material constants, if and only if the resultant force on the hole boundary vanishes and provided constant body forces. In other words, the explicit dependence of stress on Poisson's ratio is derived for the case when these conditions are not met because of unbalanced forces acting on internal boundaries.

The potential equation of the stress sum in (7) is for convenience transformed, given:

$$\Delta I_\sigma = \frac{\partial^2 I_\sigma}{\partial x^2} + \frac{\partial^2 I_\sigma}{\partial y^2} = 0 \quad \Rightarrow \quad \frac{\partial^2 I_\sigma}{\partial y^2} = -\frac{\partial^2 I_\sigma}{\partial x^2} \tag{8}$$

In addition, regarding the stress components shown in (5), by applying the Laplacian and substituting (10), the following equation may be given:

$$\Delta\sigma_{xx} = \frac{\partial^2 (\Delta\phi)}{\partial y^2} = \frac{\partial^2 I_\sigma}{\partial y^2} \tag{9}$$

The inconvenient term in Eq. (9), will be replaced by its equal given in (8), to obtain also the B-MCE for the stress component in the x-direction:

$$\Delta\sigma_{xx} = -\frac{\partial^2 I_\sigma}{\partial x^2} \tag{10}$$

By cyclic permutation of the indices, the stress component in the y-direction is obtained:

$$\Delta\sigma_{yy} = -\frac{\partial^2 I_\sigma}{\partial y^2} \tag{11}$$

while for the tangential stress, a direct application of

https://doi.org/10.1017/jmech.2015.93 Published online by Cambridge University Press

the Laplacian is used on the corresponding component (σ_{xy}) in (5):

$$\Delta\sigma_{xy} = -\frac{\partial^2(\Delta\phi)}{\partial x\partial y} = -\frac{\partial^2 I_\sigma}{\partial x\partial y} \tag{12}$$

Notice that, Eqs. (10), (11) and (12) are other writings of B-MCE given in (4) provided that the body forces are constant. It is worth mentioning that these equations may follow directly from the equilibrium equations (1), when the body forces are omitted there [32-34].

In summary, the following may also be noted. In the case of constant body forces, the B-MCE for plane stress and plane strain is the same and free from material constants. This characteristic is important in that any convenient isotropic material may be used to substitute for the actual material, as for example, in model experimental techniques, including photoelasticity firstly. Besides, the conditions in plane elasticity under which stress is independent of Poisson's ratio are well known. Indeed, in the absence of body forces, the B-MCE (10), (11) and (12) are governing equations of the Poisson type. They are independent of the elasticity constants, as emphasized earlier on by Muskhelishvili; and hereafter, this subject was comprehensively discussed in the work of Okumura [35]. In his work [26], Muskhelishvili has emphasized that for the elastic plane under the assumption that holes contours are free loading; the stress state does not depend on the elastic constants of the material. These are also fundamental assumptions of the Kirsch's Problem. Besides, according to this theorem, the Beltrami-Michell methodology may effectively be used for analyzing domains with cut-outs of any shape.

Moreover, the method of treatment of the required Dirichlet data by means of photoelasticity is briefly summarized. Photoelasticity is a full-field experimental model technique for stress analysis and is much easier, accurate, and more versatile. The isochromatic fringe patterns observed through the polariscope are given by the stress-optic law:

$$(\sigma_1 - \sigma_2) = 2\tau_{\max} = \frac{Nf}{t} = \kappa N \tag{13}$$

where the stresses are in the plane of the model of thickness t, N are either integer, 0, 1, 2 etc or half-order, 0.5, 1.5, 2.5 *etc*. subject to whether the polariscope is crossed or aligned. The stress-optic fringe coefficient f depends in turn of the transparent model material being used and the wave length, λ, of the transmitted light utilized to illuminate it. By definition, the boundaries which are free from external shear and normal stresses will be referred to as free boundaries. Indeed, the principal stresses are therefore either tangent or normal to the boundary [36]. It follows that at points lying on free boundaries there is only one remaining principal stress, which is tangent, while the normal one is obviously zero. Hence, boundary data required for solving the potential Eqs. (10), (11) and (12) are given straightforwardly using (13):

$$\left|(\sigma_{xx} + \sigma_{yy})_{\partial\Omega}\right| = \left|(\sigma_1 - \sigma_2)_{\partial\Omega}\right| = \kappa \cdot N(x, y)\big|_{\partial\Omega} \tag{14}$$

where the remaining principal stress is converted from the isochromatic fringe order $N(x, y)$ to obtain the boundary value everywhere; whereby $\kappa = f / t$ is a photoelastic model fringe value. Knowing the outward normal vector on the boundary surface, anywhere, the required Cartesian stress components may always be computed:

$$\begin{aligned} \sigma_{xx} &= \kappa \cdot N(x, y) \cdot \cos^2\theta \ ; \\ \sigma_{yy} &= \kappa \cdot N(x, y) \cdot \sin^2\theta \ ; \\ \sigma_{xy} &= -\kappa \cdot N(x, y) \cdot \sin\theta \cdot \cos\theta \end{aligned} \tag{15}$$

and which are necessary to solve the set of the B-MCE (10), (11) and (12). Obviously, the angle, θ, represents the direction (or slope) at the considered boundary point.

3. FINITE DIFFERENCE DISCRETIZATION OF THE PROBLEMS

The most direct way to solve BM-BVP numerically is through the use of finite difference approximations. The FDM usually imposes a regular grid on the region of interest. However, it has a limitation that the difference grids are restricted to be the coordinate lines, which are parallel to the coordinate axes. Therefore it is not useful on the domain grids with irregular boundaries which occur in the majority of the practical problems (see the application examples afterwards). For this purpose, a numerical differentiation technique is introduced, as has been proposed by Shortley and Weller [37], however improved. Specifically, we need to consider a 5-point star (at unequal arms) in the finite difference mesh. For homogeneous second order derivatives, we represent each distance (arm length) by αh, where $\alpha\{\alpha \in]0, 1]\}$ is a fraction of the standard spacing h, for points close to the boundary. It is obviously, for grid points away from the boundary $\alpha = 1$. On the other hand, for mixed derivatives with respect to x and y, a 45° skewed grid is opted for, in order to preserve the 5-Point differentiation scheme as used by homogeneous derivatives. The grid fractions parameter, in this case β, regulates the distances between the 4 *cardinal* points in the 45°- rotated grid. In fact, for each derivative type, 5 coefficients, $a(\alpha_k)$, $b(\beta_k)$ for k = (0, 1, 2, 3, 4), have to be calculated for each point (i, j) and, and therefore, for each algebraic finite difference equation. Again, for points far from the boundary, it may evidently be assumed: $\alpha_k = \beta_k = 1$. Henceforth, a varying 5-point stencil is systematically used for the purpose, allowing so the discretization of both homogeneous and mixed second order partial derivatives occurring in the right-hand-side of the Beltrami-Michell equations. In addition, this improved Shortley-Weller method is a practical proposal to greatly enhance the approximation with respect to the experimental meas-

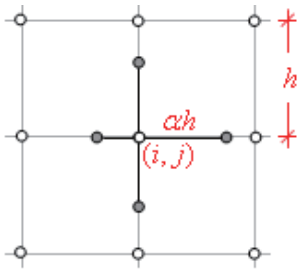
https://doi.org/10.1017/jmech.2015.93 Published online by Cambridge University Press

ured values at precise locations, especially, on domain of arbitrary geometry.

Therefore, in order to approximate the solution of Laplace Eq. (7) and Poisson Eqs. (10) ~ (12), a centered finite difference formula for the second derivative is used for both. Let Φ be a generic grid variable used for the approximation of ϕ. Using the 5-point-stencil formula, for the unequal armed star, the symbolical, following compact algebraic equation at each stencil-centre can be written, given:

$$\sum_{k=\{0,1,2,3,4\}} c_k \Phi_k = \begin{cases} 0 & Laplace \\ f\,|_{(k=0)} & Poisson \end{cases} \tag{16}$$

In this equation, the coefficients c_k regulate the spacing (as weighting) to the boundary $\partial\Omega$ and f represents each right-hand-side of the stress component Eqs. (10), (11) and (12). It should further be emphasized that for homogeneous derivatives, the coefficients of the finite difference equations are designated by: $c_k = a_k$; as shown below in sketch (a). The Shortley-Weller coefficients will be distinctly expressed as:



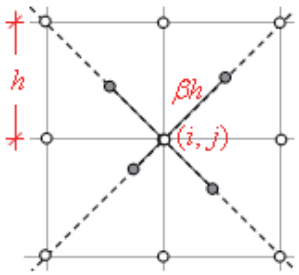
(a)

$$a_1 = \frac{1}{h^2 \cdot \alpha_1(\alpha_1 + \alpha_3)}, \quad a_2 = \frac{1}{h^2 \cdot \alpha_2(\alpha_2 + \alpha_4)}$$

$$a_3 = \frac{1}{h^2 \cdot \alpha_3(\alpha_3 + \alpha_1)}, \quad a_4 = \frac{1}{h^2 \cdot \alpha_4(\alpha_4 + \alpha_2)}$$

$$a_0 = -\sum_{k=1}^{4} a_k \tag{17}$$

Crucial undertaking is to formulate the discretization of the right-hand-side of the Poisson's equation of the shear stress (12) at irregular boundaries. The motivation of the following finite difference scheme is to produce an accurate approximation treating mixed derivatives. However, close to the boundary, customary the approximation of the second order mixed derivatives requires a 9-point stencil. This task is not easy to handle in regard to the aimed "automatization" of the solver and related the computational procedure. A transformation by rotation (45°) of the grid (stencil) to obtain also a 5-point formula is suggested. In this way, the 2-Dimensional Taylor's theorem, according to the approximation of mixed derivatives, leads to a similar form of Shortley-Weller's coefficients above. Therefore, in a 45°-skewed stencil as shown below (Sketch *b*), its finite difference coefficients ($c_k = b_k$) can be expressed explicit as follows:



(b)

$$b_1 = \frac{1}{2h^2 \cdot \beta_1(\beta_1 + \beta_3)}, \quad b_2 = \frac{-1}{2h^2 \cdot \beta_2(\beta_2 + \beta_4)}$$

$$b_3 = \frac{1}{2h^2 \cdot \beta_3(\beta_3 + \beta_1)}, \quad b_4 = \frac{-1}{2h^2 \cdot \beta_4(\beta_4 + \beta_2)}$$

$$b_0 = -\sum_{k=1}^{4} b_k \tag{18}$$

Note that by definition, the irregular 5-point-Star is present when at least one of its star boughs becomes smaller than the mesh size h. The irregular finite difference star is the more general one, while for the regular ones one requires $\alpha_k = \beta_k = 1$.

Consider the resulting linear system that arises from the discretization of such elliptic boundary value problems depicted as: $Ax = b$, where A is a $n \times n$-matrix, x and b are vectors. The main advantages of direct methods for solving systems of linear equations are their generality and robustness [38]. Direct methods solve the problem by a finite sequence of operations, and are attractive since in theory they yield the "exact" solution to the finite difference equations system, whereas commonly used methods seek to approximate the solution by iterative procedures [39]. To sum up, in the present algorithm used direct method is version of Gaussian elimination and involves the explicit factorization of the system matrix A into a product of lower L, upper U triangular and diagonal matrices, such that the product holds: $A = LDU$. Furthermore, the advantages of this method are not only its numerical strength but also the fact that it always guaranties a solution for different complex problems without the necessity of a convergence criterion (see [40]). According to our experience, while exact experimental values are involved, which have been measured at precise location on the boundary, iterative and relaxation methods have been shown to be unsuitable, with noticeable loss of accuracy in their results.

4. METHOD VALIDATION AND ANALYSIS

The stress distributions around a central hole can be estimated for the simple case of an infinitely wide plate subjected to tensile loading. We assume that the state of stress in such weakened plates is approximately plane stress, providing that the plate thickness $t << a$; compared to the hole radius a (see Fig. 1: Infinite Kirsch's domain). Besides, exact rigorous solution for the finite panel has not been obtained yet (as sketched in Fig. 1: Finite Beltrami-Michell's domain).

https://doi.org/10.1017/jmech.2015.93 Published online by Cambridge University Press

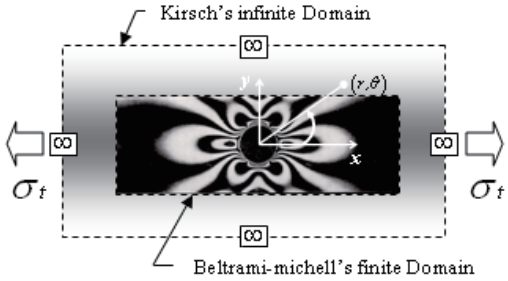


Fig. 1 Kirsch's infinite plate and plate with finite width of Beltrami-Michell.

However, for a plate under uniaxial tensile stress σ_t with the origin of the coordinates at the center of the circular hole (diameter $2a$), the Kirsch's analytical equations for the stress tensor components are usually formulated in polar coordinate systems [41]. For the sake of convenience, the algorithm is general implemented for rectangular coordinates; and therefore a transformation of stress is required. The transition to the Cartesian coordinate system is performed with the help of the two dimensional stress transformation equations and some trigonometric functions. It should be noted that the counter-clockwise nature of the angle θ has already been taken into consideration in the equations listed below. However, the overall Cartesian stress distributions are given in the closed form solution for a wide plate with a small central circular hole:

$$\sigma_{xx} = \sigma_t + \frac{\sigma_t}{2} \cdot \frac{a^2}{r^2}\left(1 + \frac{3a^2 + 10x^2}{r^2} - F + G\right) \tag{19}$$

$$\sigma_{yy} = \frac{\sigma_t}{2} \cdot \frac{a^2}{r^2}\left(3 - \frac{3a^2 + 18x^2}{r^2} + F - G\right) \tag{20}$$

$$\tau_{xy} = \sigma_t \cdot \frac{a^2 xy}{r^4}\left(3 - \frac{2(3a^2 + 4x^2)}{r^2} + \frac{12a^2 x^2}{r^4}\right) \tag{21}$$

where $r^2 = x^2 + y^2$ is the square of the distance measured from the hole center to an arbitrary point (x, y) of the plate, $F = 8x^2(3a^2 + 2x^2)/r^4$ and $G = 24\ a^2x^4)/r^6$; and σ_t is the magnitude of the remotely applied tensile stress at infinity. Herewith, we can obtain the Cartesian components of the stress in xy-plane at any point around the boundary of the circular hole.

Two experiments have been performed in this application section for validation. Firstly, the results of the Beltrami-Michell methodology have been compared with those obtained using the closed form solution of the classical problem of a wide thin plate weakened by a small central hole. Secondly, the analysis which was carried out of a photoelastic strip weakened by a central circular hole allows the comparisons of the methodology results with the experimental ones. That is why a direct comparison of the exact solutions for an infinite and a finite panel are necessary.

4.1 Application on a Stressed Kirsch's Infinite Plate

At first, the wide panel subjected to a uniaxial uniform distributed tensile stress σ_t in x-direction, given in Fig. 1 (infinite Kirsch's domain), is taken into consideration. The dimensions are selected of such a way that they can be considered as infinite wide plate; since the ratio of plate half-width to hole diameter $w/2a$ is greater than four. The stress levels outside the perturbed region are therefore close to the nominal applied stress levels σ_t (remote or far-field stress). Recall that, the inner surface of the hole is stress free which is consistent with the principal stresses at free boundary $(r = a)$:

$$\begin{aligned} &\sigma_{rr}\ (r = a, \theta) = 0\,; \\ &\sigma_{\theta\theta}\ (r = a, \theta) = \sigma_t\big(1 - 2\cos(2\theta)\big)\,; \\ &\tau_{r\theta}\ (r = a, \theta) = 0 \end{aligned} \tag{22}$$

where only the hoop stress acts varying around the boundary of the hole. On the other hand, a coordinate transformation of the non-zero component $\sigma_{\theta\theta}$ leads to the Cartesian stresses acting on the hole edge:

$$\begin{aligned} &\sigma_{xx}(r = a, \theta) = \sigma_{\theta\theta}\sin^2\theta\,; \\ &\sigma_{yy}(r = a, \theta) = \sigma_{\theta\theta}\cos^2\theta\,; \\ &\tau_{xy}(r = a, \theta) = -\sigma_{\theta\theta}\sin\theta\cos\theta \end{aligned} \tag{23}$$

Equations (23) show that the stresses in Cartesian coordinates σ_{xx}, σ_{yy} and τ_{xy} along the circular edge of the hole are functions only of both the tangential stress $\sigma_{\theta\theta}$ and the angle θ. Moreover, the required Dirichlet conditions (23) are used for solving the BM-BVP. As a result, a good agreement was observed in all the stress profiles between the closed form solution results of Kirsch and the numerical results of the used Beltrami-Michell methodology (Figs. 2 and 3).

The variations observed between these two approaches, as outlined above (Figs. 2 and 3), may presumably be attributed to the discussed numerical errors in section 3, as well as to the assumption of infinitely extended plate, which of is fundamental for the closed form solution. With more sophisticated numeric codes, the accuracy level of the results can certainly be higher until close to the analytical ones. To be emphasized moreover that the ultimate goal of this paper is rather to shown the methodology analyzing the stress tensor field of irregular shaped domains, which may in addition be weakened by cut-outs. Any other possible refinement in image processing to acquire more correctly the Dirichlet data, or improved numerical treatments of the problem, and other details, this will a matter of the end-user.

For a circular centred hole in a rectangular plate, the maps of the Beltrami-Michell stress separation were shown on the left hand side, and the analytically obtained maps were shown on the right hand side in figures (Figs. 4, 5, 6 and 7) below. It was found that the numerically obtained stress contours agree with those analytically computed ones; confirming therefore the feasibility of the present Beltrami-Michell stress evaluation and separation methodology.

https://doi.org/10.1017/jmech.2015.93 Published online by Cambridge University Press

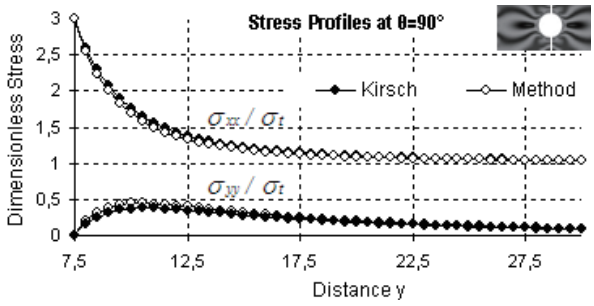


Fig. 2 Dimensionless Stress profiles along the *y*-Direction

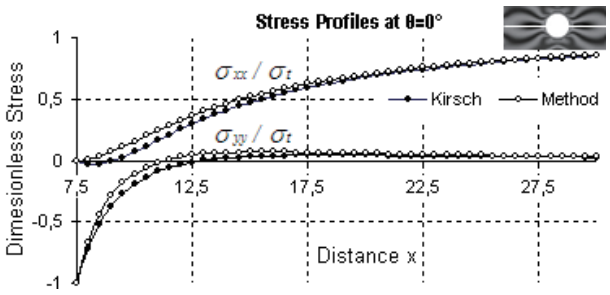


Fig. 3 Dimensionless Stress profiles along the *x*-Direction.

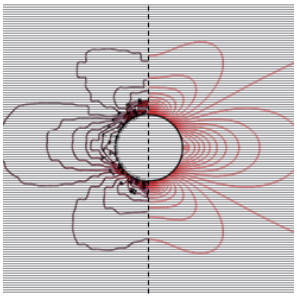


Fig. 4 Contours of Stress: σ_{xx}.

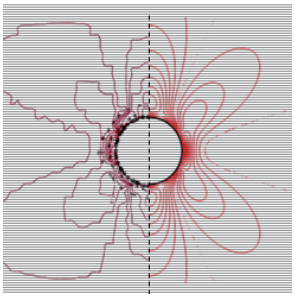


Fig. 5 Contours of Stress: σ_{yy}.

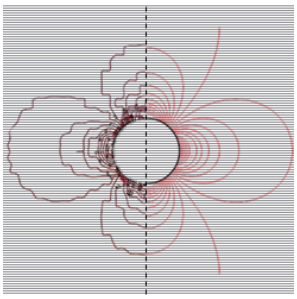


Fig. 6 Contours of Stress: σ_{xx} σ_{yy}.

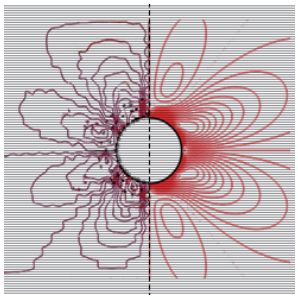


Fig. 7 Contours of Stress: σ_{xy}.

4.2 Application on a Stressed Beltrami-Michell's Finite Plate with Hole

In the second experiment, the specimen selected for validating the proposed technique is a finite width transparent polycarbonate tension member with a central circular hole. The isochromatic fringe patterns photograph for this model is shown in (Fig. 8.) (see Frocht [42]; pp 231–232). However, attempt will be made to quantify the stress distributions associated with isochromatic fringe patterns as a means to collect the Dirichlet experimental data on the boundaries. In the figure below, the fringe values and their signs have been determined and marked on the outside boundaries of the stripe without further difficulty. A negligible deviation was found one being opposite sides of the specimen due to a load small eccentricity of course. According to the Saint-Venant principle, small error in fringe order may also be shown to be of negligible importance, at least for this purpose. Furthermore, in the context of boundary value problems Frocht has devoted one chapter in his work (see Frocht [43]; Chapter 8) for the algebraic harmonisation for solving the Laplace equation of the stress sum by an iterative relaxation procedure, credited to Liebmann and known furthermore as the Liebmann relaxation procedure [44]. In his work Frocht has emphasized that small errors of location and magnitude of the boundary values decay rather quickly in the vicinity of the boundary, having no influence on the global results far away. Besides, the used input subroutine for this purpose adopts a cubic B-spline curve that produces smooth boundary values with least oscillatory shapes. This is needed furthermore for the interpolation at FDM-grid intersection (missing) points with the boundary. The boundary values in magnitude and location are beforehand recorded by means of digitizing tablet; a common peripheral device.

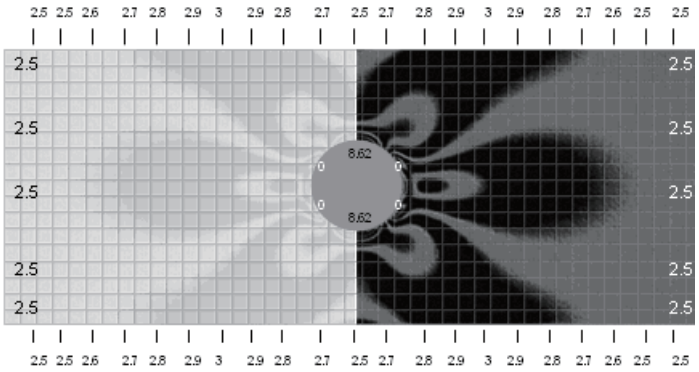


Fig. 8 Isochromatic fringes data simulating the Dirichlet's data of the problem.

The distribution of the isochromatic fringes at the periphery of a circular hole is analyzed and separately presented in (Fig. 9) for convenience. On the hole circumference, they are four zones symmetrically opposed including two of compression (0-B-0) and two of tension (0-A-0); see photograph in medallion (Fig. 9). Those zones are joined together by *isotropic points* of zero stress, separating tensile stress regions from compressive stress ones. Noticing that a singular point is an isotropic point at which the stresses are zero, while at isotropic points the principal stresses are equal in all directions, *i.e.* hydrostatic conditions. The directional properties of this singular point of zero stress, "0", located approximately at 30 degrees from the vertical centreline will be best understood when we refer to the isoclinic and isostatic diagrams as shown by (see Frocht [42]; pp 214). However, the maximum isochromatic order (at point A) was determined by plotting the fringe order against the distance from one of the edge at the minimum section and extrapolating this curve to the true edge of the hole. It was necessary to use an enlargement since the fringes were very fine and close

https://doi.org/10.1017/jmech.2015.93 Published online by Cambridge University Press

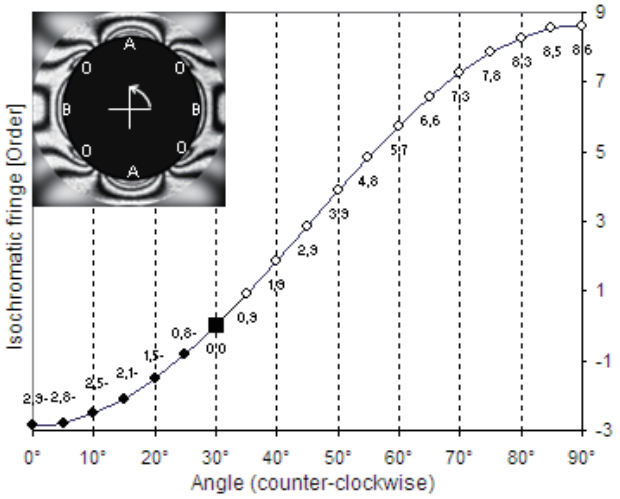


Fig. 9 Fringes at the periphery a quarter of hole vs. angle.

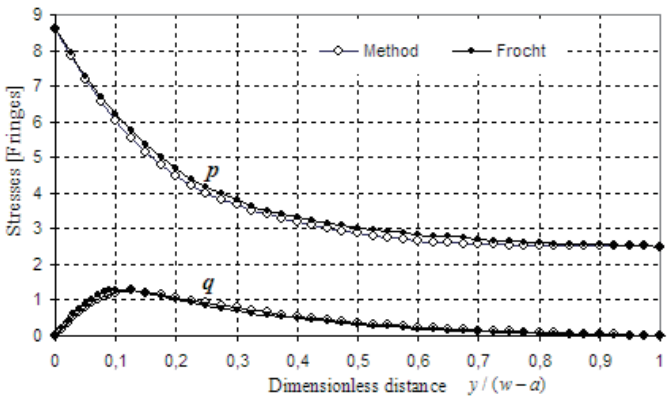


Fig. 10 Principal Stress Profiles [Fringes] along the y-Direction.

together. photoelasticity always delivers complete information on the stress at load free boundary, because of the direction of stress which is furthermore known, since the physical boundary or edge is a stress direction itself.

It shou1d be noted, though, that photoelastic resu1ts are expressed in terms of fringes. Assuming e1astic conditions and similitude between model and prototype, it is not necessary that these fringe values be converted into stresses for this purpose. Therefore, the fringe orders can also be assumed as boundary values on both edges of plate and hole. On the other hand, due to the material symmetry and symmetrical loading condition, the symmetry planes are principal ones, and therefore free from shear stress. For convenience we will denote the particular values of both σ_{xx} and σ_{yy}, acting on such principal planes, by p and q, as it was done in the reference work. Consequently, the algebraically maximum stress will be denoted by p and the minimum one by q. However the maximum shear stress, equals the radius of the Mohr's Circle, is denoted by $\tau_{\max} = (p - q)/2$.

The stress concentration or dimensionless stress predicted in (Fig. 2) decays rather quickly away from the hole. Therefore, this solution can be used for non-infinite plates, provided that the edges of the plate are sufficiently far from the hole that the stresses on the edges are approximately equal to the remote stress field. If this is not the case, alternative solution by Howland [45] may be used. Howland derived semi-analytical expression for the stress concentration factors at the edge of a symmetric hole of diameter $2a$ in a plate of finite width $2w$. Many others semi-analytical formulae are proposed in text-books by Perteson [46] and by Warren *et al*. [47]. The simplest and most conservative formula is given by Boresi [48], as shown in Eq. (24) below.

$$\frac{\sigma_{\max}}{\sigma_{av}} \approx \frac{3\kappa - 1}{\kappa + 0.3} \tag{24}$$

where κ ($= w/a$) is the ratio (width of strip/diameter of hole) and σ_{av} is the average stress over the weakened cross-sectional area containing the hole. The following empirical equations for the stress concentration factor K_{scf} give results agreeing approximately with the most experimental test and FEA results:

$$\frac{\sigma_{\max}}{\sigma_{av}} \approx 3 - 3.13\left(\frac{a}{w}\right) + 3.66\left(\frac{a}{w}\right)^2 - 1.53\left(\frac{a}{w}\right)^3 \tag{25}$$

Values shown in Table 1 should justify the fringe order extrapolation, across the transverse section of symmetry, on the free boundary point of the hole centred in the stripe ($a/w = 0.3$).

Table 1 Abstract of normalized stress of stripes weakened by central hole

Eq. (24)	2.48	
Eq. (24)	2.48	
Howland	2.48	
Average	2.48	2.30 (Photoelasticity)

5. CONCLUSIONS

In order to overcome the heavy and fastidious analysis inherent in the displacement or complex variable formulation, used to obtain eventually the stress field [49], the direct formulation in terms of stress is an adequate straightforward proposal. In this paper the developed hybrid method uses the measured surface stresses and the Beltrami-Michell Methodology to determine the full-field stress tensor in the interior of any irregular two-dimensional elastic domain that can either be simple or multiply connected. The successful use of such hybrid method can thereby reduce the amount of measurements required, increase the accuracy of numerical results and permit the prompt determination of the complete stress distributions within domains weakened by irregular holes. As shown, the algorithm of stress analysis is straightforward, shortens the com-

https://doi.org/10.1017/jmech.2015.93 Published online by Cambridge University Press

putational time and creates favourable condition for automatic hybrid technique of course. Quite often, the results of a finite element analysis require an experimental validation by important problems; which is almost achieved by this method. When meticulously carried out, the presented methodology advanced the finite element analysis with one more advantage that the results are simultaneously validated.

ACKNOWLEDGEMENTS

We gratefully acknowledge financial support from: Ministère de l'Enseignement Supérieur et de la Recherche Scientifique, Algeria, under grant agreement No. J0301920130020.

The authors would also like to sincerely thank both Miss Khadija Safer and Mr Touhami Baki, for reading our paper and for providing valuable advice.

REFERENCES

1. Kirsch, G., "Die Theorie Der Elastizität Und Die Bedürfnisse Der Festigkeitslehre," *Zeitschrift Des Vereins Deutscher Ingenieure*, **29**, pp. 797–807 (1898).
2. Kolosov, G. V., "On the Application of Complex Functions Theory to a Plane Problem of the Mathematical Theory of Elasticity," Ph.D. Dissertation, Dorpat (Yuriev) University (1909).
3. Inglis, C. E., "Stresses in a Plate Due to the Presence of Cracks and Sharp Corners," *Transactions of the Institute of Naval Architects*, **55**, pp. 219–230 (1913).
4. Howland, R., "On the Stresses in the Neighbourhood of a Circular Hole in a Strip Under Tension," *Philosophical Transactions of the Royal Society of London, Series A*, **229**, pp. 49–86 (1930).
5. Durelli, J. and Murray, W. M., "Stress Distribution Around a Circular Discontinuity in Any Two Dimensional System of Combined Stress," *Proceedings of the 14th Semi-Annual Eastern Photoelasticity Conference,* Yale University, New Haven (1941)
6. Durelli, J. and Murray, W. M., "Stress Distribution Around an Elliptical Discontinuity in Any Two-Dimensional, Uniform and Axial System of Combined Stress," *Proceedings of the Society for Experimental Stress Analysis*, **1**, pp. 19–31 (1943).
7. Heywood, R. B., *Designing by Photoelasticity*, Chapman & Hall, London (1952).
8. Kawadkar, D. B., Bhope, D. V. and Khamankar, S. D., "Evaluation of Stress Concentration in Plate with Cut-Out and Its Experimental Verification," *International Journal of Engineering Research and Applications*, **2**, pp. 566–571 (2012).
9. Mohan Kumar, M., Rajesh, S., Yogesh, H. and Yeshaswini, B. R., "Study on the Effect of Stress Concentration on Cut-out Orientation of Plates with Various Cut-outs and Bluntness," *International Journal of Modern Engineering Research*, **3**, pp. 1295–1303 (2013).
10. Nagpal, S., "Optimization of Rectangular Plate with Central Square Hole Subjected to In-Plane Static Loading for Mitigation of SCF," *International Journal of Engineering Research and Technology*, **1**, pp. 1–8 (2012).
11. Nilugal, R. and Hebbal, M. S., "A Closed-Form Solution for Stress Concentration Around a Circular hole In a Linearly Varying Stressed Field," *International Journal of Materials Engineering and Technology*, **4**, pp. 37–48 (2013).
12. Singh, A. K., Rashid, A. and Singh, V. K., "An Infinite Plate Weakened by a Circular Hole," *International Journal of Engineering and Science Invention*, **2**, pp. 32–39 (2013).
13. Mallikarjun, P., Dinesh, K. I., Parashivamurthy, "Finite Element Analysis of Elastic Stresses around Holes in Plate Subjected to Uniform Tensile Loading," *Bonfring International, Journal of Industrial Engineering and Management Science*, **2**, pp. 136–142 (2012).
14. Shastry, P. and Venkateswara, Rao G., "Studies on Stress Concentration in Tensile Strips with Large Circular Holes," *Composite Structures*, **19**, pp. 345–349 (1984).
15. Isida, M., "On the Tension of a Strip with a Central Elliptic Hole," *Transactions of the Japan Society of Mechanical Engineers*, **21**, p. 514 (1955).
16. Kotousov, Wang C. H., "Three-Dimensional Stress Constraint in an Elastic Plate with a Notch," *International Journal of Solids and Structures*, **39**, pp. 4311–4326 (2002).
17. Yang, Z., Kim, C. B., Cho, C. and Beom, H. G., "The Concentration of Stress and Strain in Finite Thickness Elastic Plate Containing a Circular Hole," *International Journal of Solids and Structures*, **45**, pp. 713–731 (2008).
18. Dharmin, P., Khushbu, P. and Chetan, J., "A Review on Stress Analysis of an Infinite Plate with Cut-Outs," *International Journal of Scientific and Research Publications*, **2**, pp. 1–7 (2012).
19. Pilkey, W. D., *Peterson's Stress Concentration Factors*, Wiley, New York (1997).
20. Sokolnikoff, I. S., *Mathematical Theory of Elasticity*, McGraw-Hill, New York (1956).
21. Love, A. E. H., *A Treatise on the Mathematical Theory of Elasticity*, 4th Ed., Cambridge University Press, Cambridge (1927).
22. Abdou, M. A. and Monaquel, S. J., "An Integral Method to Determine the Stress Components of Stretched Infinite Plate with a Curvilinear Hole," *International Journal of Research and Reviews in Applied Sciences*, **6**, pp. 353–358 (2011).

https://doi.org/10.1017/jmech.2015.93 Published online by Cambridge University Press

23. Churchill, R. V., *Complex Variables and Applications*, McGraw-Hill, New York (1960).
24. England, A. H., *Complex Variable Methods in Elasticity*, John Wiley, New York (1971).
25. Savin, G. N., *Stress Concentration Around Holes*, Pergamon Press, New York (1961).
26. Muskhelishvili, N. J., *Some Basic Problems of the Mathematical Theory of Elasticity*, Wolters-Noordhoff, Groningen (1963).
27. Boresi, P., Chong, K. P. and Lee, J. D., *Elasticity in Engineering Mechanics,* 3rd Ed., John Wiley and Sons, Inc., New Jersey (2011).
28. Lurie, I., *Theory of Elasticity*, 4th Ed., translated by Belyaev, Springer, Berlin (2005).
29. Durelli, J., Phillips, E. A. and Tsao, C. H., *Introduction to the Theoretical and Experimental Analysis of Stress and Strain*, McGraw-Hill, New York, pp. 126–131 (1958).
30. Ramesh, K., *Digital Photoelasticity*, Springer, New York (2000).
31. Rezini, D., "Randisochromaten Als Ausreichende Information Zur Spannungstrennung Und Spannungsermittlung," "Boundary Isochromatics as Sufficient Information for the Stress Separation and Stress Determination," PhD. Dissertation, Tech. University of Clausthal, (TUC), Germany (1984).
32. Meleshko, V. V., "Selected Topics in the History of the Two-Dimensional Biharmonic Problem," *Applied Mechanics Reviews*, **56**, pp. 33–85 (2003).
33. Vihak and Rychagivskii, "Solution of a Three-Dimensional Elastic Problem for a Layer," *International Applied Mechanics*, **38**, pp. 1094–1102 (2002).
34. Tokovyy, V. and Ma, C. C., "Analytical Solutions to the 2D Elasticity and Thermoelasticity Problems for Inhomogeneous Planes and Half-Planes," *Archive of Applied Mechanics*, **79**, pp. 441–456 (2009).
35. Okumura, I., "The Mathematical Theory of Thick and Thin Elastic Rectangular Disks in the States of Plane Stress and Plane Strain," *Memoirs of the Kitami Institute of Technology*, **33**, pp. 9–19 (2002).
36. Kuske, A. and Robertson, G., *Photoelastic Stress Analysis*, John Wiley & Sons, New York (1974).
37. Shortley, H. and Weller, R., "The Numerical Solution of Laplace's Equation," *Journal of Applied Physics*, **9**, pp. 334–348 (1938).
38. Buzbee, L., Golub, G. H. and Nielson, C. W., "On Direct Methods for Solving Poisson's Equations," *SIAM Journal on Numerical Analysis*, **7**, pp. 627–656 (1970).
39. Saad, Y., *Iterative Methods for Sparse Linear Systems*, 2nd Ed. Society for Industrial and Applied Mathematics Philadelphia (2003).
40. Press, W. H., Teukolsky, S. A., Vetterling, W. T. and Flannery, B. P., *Numerical Recipes: The Art of Scientific Computing*, 3rd Ed., Cambridge University Press, Cambridge (2007).
41. Timoshenko, S. P. and Goodier, J. N., *Theory of Elasticity*, 3rd Ed., McGraw Hill, New York (1970).
42. Frocht, M., *Photoelasticity*, 1, John Wiley & Sons, New York (1941).
43. Frocht, M., *Photoelasticity*, 2, John Wiley & Sons, New York (1948).
44. Liebmann, H., "Die Angenäherte Ermittlung Harmonischer Funktionen Und Konformer Abbildungen," *Sitzungsberichte der Bayerischen Akademie der Wissenschaften Mathematisch-Physikalische Klasse*, pp. 385–416 (1918).
45. Howland, R., "On the Stresses in the Neighbourhood of a Circular Hole in a Strip Under Tension," *Philosophical Transactions of the Royal Society of London, Series A*, **229**, pp. 49–86 (1930).
46. Peterson, R. E., *Stress Concentration Factors*, John Wiley & Sons, Inc., New York (1974).
47. Warren, C. Y. and Richard, G. B., *Roark's Formulas for Stress and Strain*, 7th Ed., McGraw-Hill, New York (2002).
48. Boresi, P., Schmidt, R. J. and Sidebottom, O. M., *Advanced Mechanics of Materials*, 5th edition, John Wiley and Sons, Inc., New York (1993).
49. Gao, X-L. and Rowlands, R. E., "Hybrid Method for Stress Analysis of Finite Three-Dimensional Elastic Components," *International Journal of Solids and Structures*, **37**, pp. 2727–2751 (2000).

(Manuscript received March 13, 2014,
accepted for publication August 17, 2015.)

https://doi.org/10.1017/jmech.2015.93 Published online by Cambridge University Press